Journal of Solid Mechanics Vol. 8, No. 4 (2016) pp. 744-755

Ductile Failure and Safety Optimization of Gas Pipeline

P. Zamani, A. Jaamialahmadi *, M. Shariati

Department of Mechanical Engineering, Ferdowsi University of Mashhad, Mashhad, Iran

Received 11 July 2016; accepted 15 September 2016

ABSTRACT

Safety and failure in gas pipelines are very important in gas and petroleum industry. For this reason, it is important to study the effect of different parameters in order to reach the maximum safety in design and application. In this paper, a three dimensional finite element analysis is carried out to study the effect of crack length, crack depth, crack position, internal pressure and pipe thickness on failure mode and safety of API X65 gas pipe. Four levels are considered for each parameter and finite element simulations are carried out by using design of experiments (DOE). Then, multi-objective Taguchi method is conducted in order to minimize x and y coordinates of Failure Assessment Diagram (FAD). So, desired levels that minimize the coordinates and rises the possibility of safety are derived for each parameter. The variation in FAD coordinates according to the changes in each parameter are also found. Finally, comparisons between the optimum design and all other experiments and simulations have shown a good safety situation. It is also concluded that the more design parameters close to optimum levels, the better safety condition will occur in FAD. A verification study is performed on the safety of longitudinal semi-elliptical crack and the results has shown a good agreement between numerical and experimental results.

Keywords : Semi-elliptical crack; Finite element analysis; Taguchi method; Failure assessment diagram.

1 INTRODUCTION

THE presence of defects in materials especially metals used in the construction of vessels are inevitable. Failure in cylindrical vessels occurs due to widespread presence of cracks. One of the functions of cylindrical vessels is in oil and gas industry. Therefore, considering the fracture mechanics parameters is important in the design of these structures. Estimates for stress intensity factors for internal surface cracks in pressurized cylinders are achieved by Underwood [1]. He did not considered the effect of thickness in their estimation. Raju and Newman [2] presented stress intensity factor for a wide range of semi-elliptical internal and external surface cracks. Newman et al. [3] carried out an investigation to study the fracture criteria for surface and deep cracks in pressurized pipes. They verified fracture criteria with experimental results. They also presented relations for calculating fracture toughness in different cracks. Then, Liu et al. [4] made a comparison between internal and external axial cracks in cylindrical pressure vessels. They showed that the amount of stress intensity factor for internal cracks is higher than SIF amounts in external cracks. They also concluded that there is almost no difference between internal and external cracks in thin-walled cylinders. So the difference is only important in thick-walled cylinders or vessels. Lee et al. [5] evaluated tensile properties and fracture toughness of base metal, weld metal and heat affected zone. They checked the safety of a gas pipeline in different lengths and depths of cracks. In continue, Oh et al. [6] applied a local failure

*Corresponding author. Tel.: +98 5138805034.
E-mail address: jaami-a@um.ac.ir (A. Jaamialahmadi).

criterion to API X65 steel in order to predict ductile failure of full-scale pipes. Sandvik et al. [7] presented a probabilistic fracture mechanics model established from three-dimensional FEM analyses of surface cracked pipes subjected to tension load in combination with internal pressure. In their numerical models, the plastic deformations, including ductile tearing effects, are accounted for by using the Gurson-Tvergaard-Needleman model. This model is calibrated to represent a typical X65 pipeline steel behavior under ductile crack growth and collapse. Several parameters are taken into account such as crack depth, crack length and material hardening [7]. Fracture behavior of materials is evaluated using failure assessment diagrams by Pluvinage et al. [8]. According to Fedderson diagram, the safe area of the failure assessment diagram divides to three regions. They predicted the type of fracture in two pipes of different materials. They concluded that the pipe made up of cast iron is prone to brittle fracture and the steel pipe is going to experience elastic-plastic fracture. They also showed that axial crack (semi-elliptical or longitudinal cracks) are more critical than hoop (circumferential) cracks. Ductile fracture mechanism of API X65 buried pipes including crack initiation and propagation is studied using the extended finite element method (XFEM) [9]. In addition, they considered the effects of different crack configurations, damage initiation and evolution criteria [9]. Ghajar et al. [10] also studied the effect of anisotropy and triaxiality factor on ductile failure of X100 steel pipeline. Their main investigation relates to performing an extensive fractography by SEM to study the fracture surfaces and they concluded that triaxiality causes sooner failure occurrence. Sharma et al. [11] carried out a numerical investigation using extended finite element Method (XFEM) in order to compute stress intensity factors (SIFs) in a part with a semi-elliptical part through thickness axial crack. They compared their results with finite element method (FEM). Dimic et al. [12] conducted three dimensional numerical study on calculating J-integrals for axial external cracks in gas and oil drilling rig pipelines. They also measured crack mouth opening displacement in experimental investigation and considered fracture initiation and plastic collapse as failure mechanisms.

Previous investigations mostly based on the effect of different types of cracks on the safety of pipes using different failure criteria, but it is very important to perform a study to find out the effect of different parameters on the safety by considering their effects at the same time and also to achieve the safest pipe design for these parameters. In this paper, a cracked pipe in Iran's high pressure pipeline system is studied and optimized by considering the effects of five parameters on the safety and failure of the pipe. For this purpose, the effects of these parameters on safety condition is measured at the same time and also the optimum design (the safest working condition) is achieved on the basis of design of experiments (DOE) and Taguchi optimization procedure. The pipe has axial semi-elliptical crack that is initiated from both internal and external surfaces. There are some parameters that affect the safety of pipe such as crack length, crack depth, crack place, pipe thickness and internal pressure. For each factor, four levels are considered except the cracak place which is regarded as internal and external semi-elliptical cracks.

Then, a set of experiments are designed according to Taguchi's orthogonal array. Results of K_r and L_r are calculated for each experiment. According to Taguchi method, optimum level for each factor is achieved. Such optimum levels minimize K_r and L_r. So, minimized amounts of K_r and L_r improves the probability that the pipe states in the safe region of failure assessment diagram. Such optimization method has shown the interaction of each two parameter on K_r and L_r. In addition, it shows the factor that has the most effect on minimizing K_r and L_r. Numerical analysis is carried out by Abaqus software. After computing the results through finite element analysis and managing some manipulations based on BS7910 standard, the coordinate of the points are estimated and optimized in failure assessment diagram. Finally, experimental data are used used to verify the finite element results and an acceptable accordance is achieved between such results.

2 THEORY OF SAFETY LIMIT

Failure assessment diagrams (FADs) are popular tools in evaluating defects and cracks in industrial structures [13, 14]. The quality of fracture such as brittle fracture and plastic fracture (ductile failure) can be predicted using FADs. A couple of these diagrams are presented in API 579 standard [15]. FADs are categorized in three types. Higher-level FADs require more complex data but are less conservative. Fig. 1(a) shows a primary FAD based on the CTOD design curve-method [5]. The elastic-plastic fracture prediction procedure in BS 7910 is the basis of this method [16]. Fig. 1(b) is another type of FAD that is related to the lower bound of the curves obtained from data on general austenitic steel [5, 17]. Fig. 1(c) introduces FAD that is dependent to material properties and it needs more complicated parameters than the others and is less conservative. Besides that, FADs of level 1 and 2 are independent of material properties and contain universal failure assessment curves (FAC: criterion line of FAD) [5].

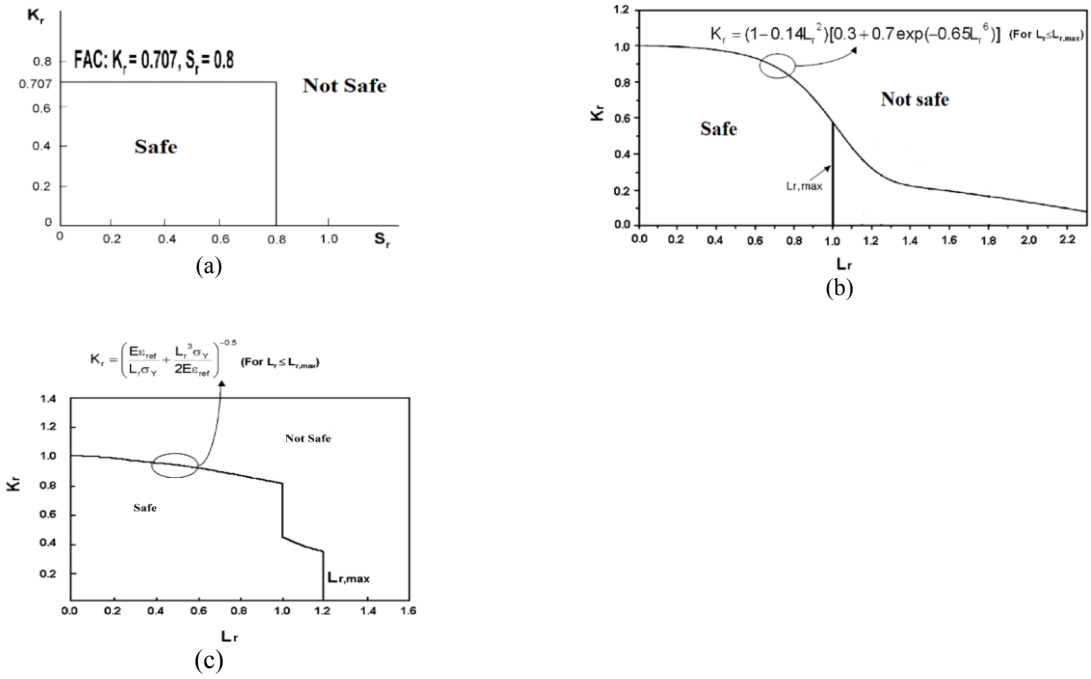

Fig.1
(a) Primary FAD based on the CTOD design curve method, (b) FAD related to the lower bound of the curves, (c) FAD independent to material properties.

According to elastic-plastic definition of the problem, *J*-integral is calculated for the pipe under preferred loading conditions by using finite element method. After obtaining the *J*-Integrals, stress intensity factors are computed using Eq. (1) [18].

$$K = \sqrt{JE} \tag{1}$$

where *J* is the amount of *J*-integral and *E* is the modulus of elasticity. Besides that, the British standard BS7910 [19] has presented a reference stress field (Eq. (2)). In continue, the points are plotted in failure assessment diagram in order to check the safety. The abscissa of coordinate system implies the ratio of reference stress to yield stress and the ordinate shows the amount of *K* for each point.

$$\sigma_{ref} = 1.2 M_s P_m + \frac{2P_b}{3(1-a'')^2} \tag{2}$$

where σ_{ref}, P_m and P_b are reference stress, hoop stress and bending stress, respectively. M_s, M_T and a'' are non-dimensional parameters that are defined as below:

$$M_s = \frac{1-\dfrac{a}{BM_T}}{1-\dfrac{a}{B}} \tag{3}$$

where *a* is the crack length and *B* is the sheet thickness. Then, M_T is defined as:

$$M_T = \sqrt{1+1.6\left(\frac{c^2}{r_i B}\right)} \tag{4}$$

where r_i and c are inner radius and crack length, respectively. The non-dimensional parameter a'' is defined by in Eq.(4), two conditions:

$$\mathrm{a}'' = \frac{\frac{a}{B}}{1+\frac{B}{c}} \quad , \quad w \geq 2(c+B)$$
$$\mathrm{a}'' = 2\left(\frac{a}{B}\right)\left(\frac{c}{\pi r_i}\right) \quad , \quad w \geq 2(c+B) \tag{5}$$

As mentioned before, J integrals are evaluated and stress intensity factors are then calculated using Eq. (1) as vertical amount of FAD. J integral is related to the energy release associated with crack growth and is a measure of the deformation intensity at a notch of a crack tip. The energy release rate along the crack front can be shown as [20]:

$$J(s) = \lim_{\Gamma \to 0} \int_{\Gamma} n.H.q \, d\Gamma \tag{6}$$

where Γ is a contour which begins from the bottom crack surface and ends on the top surface, q is a unit vector in the virtual crack extension direction and n is the outward normal to Γ. H in Eq. (6) is defined as below [20]:

$$H = WI - \sigma.\frac{\partial u}{\partial x} \tag{7}$$

where W represents strain energy. If the virtual crack advance is considered as $\lambda(s)$, the corresponding energy release is defined as Eq. (8).

$$\bar{J} = \int_{L} J(s)\lambda(s)ds = \lim_{\Gamma \to 0} \int_{A_t} \lambda(s) n.H.q \, dA \tag{8}$$

where L shows the crack front, dA is a surface element on a small tubular surface enclosing the crack tip and n is normal to this elemental surface. $\bar{J}$ can be calculated by converting the surface integral in Eq. (8) to a volume integral by introducing a contour surface A_c, outside surface A_o, side surfaces A_s and the crack surfaces A_{crack} (Fig. 2).

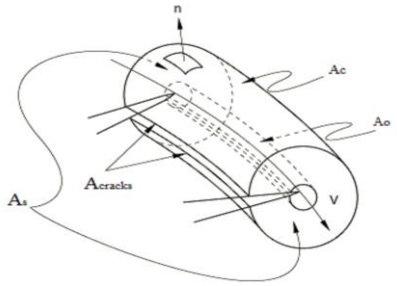

Fig.2
Surfaces encloses the crack front region.

A weight function $\bar{q}$ is defined such that the magnitude of A_c be zero and $\bar{q} = \lambda(s)q$ on A_o. So, Eq. (8) can be written as [20]:

$$\bar{J} = -\int_{A} m.H.\bar{q} \, dA - \int_{A_s + A_{crack}} t.\frac{\partial u}{\partial x}.\bar{q} \, dA \tag{9}$$

where m is the outward normal to $A = A_c + A_o + A_s + A_{crack}$ and $t = m.\sigma$ is the surface traction on side and crack surfaces. Using the divergence theorem [20]:

$$\bar{J} = -\int_V \left[H : \frac{\partial \bar{q}}{\partial x} + \left(f.\frac{\partial u}{\partial x} - \sigma : \frac{\partial \varepsilon^{th}}{\partial x} \right).\bar{q} \right] dV - \int_{A_s + A_{crack}} t.\frac{\partial u}{\partial x}.\bar{q}\, dA \tag{10}$$

where f is body force per unit volume. Calculating $J(s)$ in an arbitrary node set along crack front line can be achieved by defining $\lambda(s) = N^Q(s)\lambda^Q$, and by substituting this definition into Eq. (10), the amount of J-integral can be calculated at each node set along the crack front [20]:

$$J^P = \frac{\bar{J}^P}{\int_L N^P\, ds} \tag{11}$$

3 FINITE ELEMENT METHOD

3.1 Geometry and material

A 3D finite element model and simulation is applied for a high pressure pipe in order to estimate J-integrals. Because of symmetry in geometry and loading conditions, a quarter division of the cracked pipe is modeled. Fig. 3 shows the geometry of the modeled pipe by considering symmetry conditions. The outer radius is equal to 1.219 m.

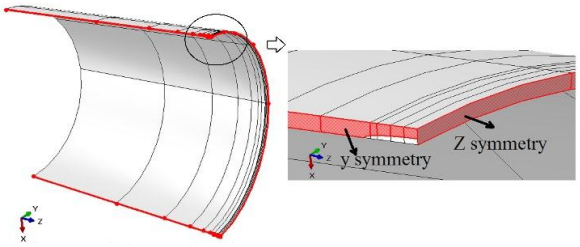

Fig.3
Geometry and symmetry conditions of pipe.

The material of the pipe is defined as elastic-plastic. Mechanical properties and elastic-plastic behavior are defined in Table 1. and Table 2., respectively [18].

Table 1
Material properties.

	E (*GPa*)	Yield stress (*MPa*)	Ultimate stress (*MPa*)
API X65 steel	210	505	611

Table 2
Plastic properties of API X65 steel [18].

Number	Yield stress (*MPa*)	Plastic strain (*MPa*)
1	505	0
2	549	0.01
3	599	0.03
4	631	0.05
5	652	0.06
6	667	0.08
7	681	0.1

8	693	0.12
9	703	0.14
10	712	0.16
11	719	0.18
12	722	0.19
13	755	0.3
14	794	0.4
15	821	0.7
16	832	0.8
17	841	0.9
18	850	1.00
19	858	1.1
20	866	1.2

3.2 Loading and meshing

A three dimensional finite element analysis is carried out using ABAQUS 6.11. Symmetry condition is considered for the pipe along longitudinal and hoop directions. So the boundary conditions are considered as symmetric along these directions. Boundary conditions along *y* and *z* axes are shown in Fig. 3 and Fig. 4.

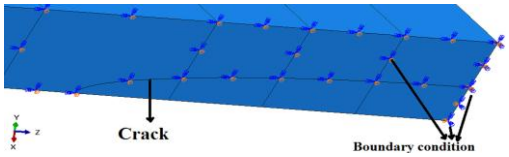

Fig.4
Boundary conditions near the crack edge.

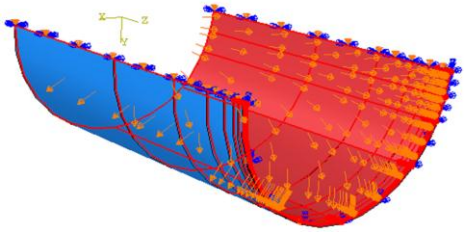

Fig.5
Loading condition (internal pressure).

Internal pressure is applied as loading conditions (Fig. 5). Because of the stress-strain singularity near the crack tip, sweep mesh command is selected for this region. The meshing in other partitions of the model is defined as structural mesh. 17035 solid elements are generated on the model and they are chosen from the Standard library and 3D stress family. In order to reduce the computation time and to achieve a better convergence in *J* integral solutions, the reduced integration option is activated. Fig. 6 shows the partitions around the crack, meshed model of the pipe and mesh density around the crack tip. Also the static solution is considered in order to analyze the model.

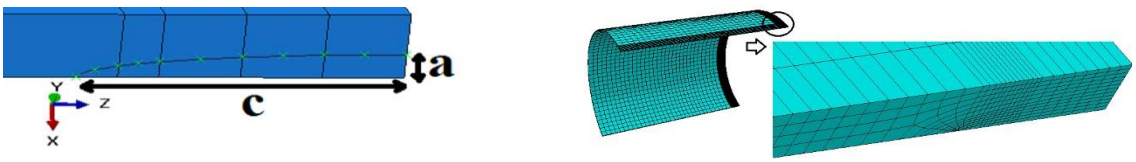

(a) (b)

Fig.6
(a)Partitions along the crack geometry, (b) Meshing in the pipe and around semi-elliptical crack.

4 OPTIMIZATION PROCEDURE

The amount of K and L in failure assessment diagrams shows the safety or unsafety of the working condition of the pressurized pipe. So, it is very important to minimize the amount of K and L in order to be sure that the pipe is in a safe condition. There are many factors that affect safety of a pressurized pipe such as internal pressure, pipe thickness, crack length, crack depth and the crack position. In this study, four levels are considered for each factor. On the basis of design of experiment (DOE), 32 experiments (simulations) are designed. Then, a finite element analysis is conducted in order to achieve J integral amounts. In continue, each point of the safety diagram is resulted from Eq. (1) and Eq. (2). The optimum experiment that minimizes coordinates of the safety diagram is found using multi-objective Taguchi method. Table 3. shows parameters that affect the amount of J integral and consequently K and L.

Table 3
Factors and their corresponding levels.

Number	Internal pressure (*MPa*)	Crack position	Pipe thickness (*mm*)	Crack length (*mm*)	Crack depth (*mm*)
Level 1	3	Internal	13.5	100	5
Level 2	4	External	14	120	6
Level 3	5		14.5	140	7
Level 4	6		15	160	8

According to Table 3, DOE orthogonal table is considered to perform finite element simulations (Table 4).

Table 4
Orthogonal array of design of experiments.

Number	Crack position (*MPa*)	Internal pressure (*MPa*)	Crack length (*mm*)	Crack depth (*mm*)	Pipe thickness (*mm*)	J integral ($MPa\sqrt{m}$)
1	Internal	3	100	5	13.5	5.55e3
2	Internal	4	100	6	14	18.64e3
3	Internal	5	100	7	14.5	2.84e4
4	Internal	6	100	8	15	6.23e4
5	Internal	3	120	5	14	8.33e4
6	Internal	4	120	6	13.5	1.59e4
7	Internal	5	120	7	15	3.27e4
8	Internal	6	120	8	14.5	7.25e4
9	Internal	4	140	5	15	9.93e3
10	Internal	3	140	6	14.5	1.13e4
11	Internal	6	140	7	14	8.32e4
12	Internal	5	140	8	13.5	9.15e4
13	Internal	4	160	5	14.5	1.47e4
14	Internal	3	160	6	15	7.39e3
15	Internal	6	160	7	13.5	8.23e4
16	Internal	5	160	8	14	5.86e4
17	External	6	100	5	15	2.39e4
18	External	5	100	6	14.5	3.10e4
19	External	4	100	7	14	2.17e4
20	External	3	100	8	13.5	2.31e4
21	External	6	120	5	14.5	5.50e4
22	External	5	120	6	15	2.29e4
23	External	4	120	7	13.5	2.37e4
24	External	3	120	8	14	1.55e4
25	External	5	140	5	13.5	2.45e4
26	External	6	140	6	14	8.3e4
27	External	3	140	7	14.5	1.15e4
28	External	4	140	8	15	3.40e4
29	External	5	160	5	14	2.73e4
30	External	6	160	6	13.5	8.91e4
31	External	3	160	7	15	1.38e4
32	External	4	160	8	14.5	4.54e4

After conducting all 32 experiments (simulations), stress distribution and J integrals are computed by means of finite element analysis. J integral amounts are calculated along contours that have the maximum level of stress. By investigating different number of contours, it is observed that the amounts of J integral are well converged by

selecting 11 contours. Stress distribution for the first and third experiments and near the crack edge are shown in Fig. 7 and Fig. 8, respectively.

After obtaining J integrals,stress intensity factors are calculated through Eq. (1), the reference stress is also calculated using Eq. (2). So there will be a set of stress intensity factor and reference stress for each experiment and it is expected that both of them to be minimized. Table 4. show the amounts of J integrals on a coordinate system which its abscissa and ordinates are stress intensity factor and reference stress, respectively.

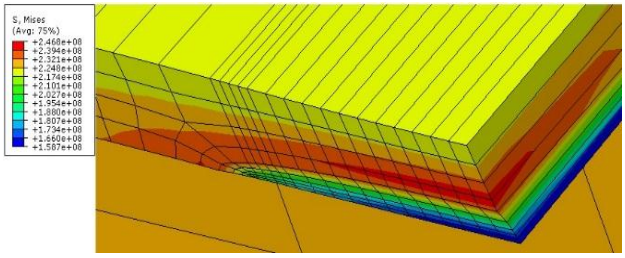

Fig.7
Stress distribution near the crack edge (1st experiment).

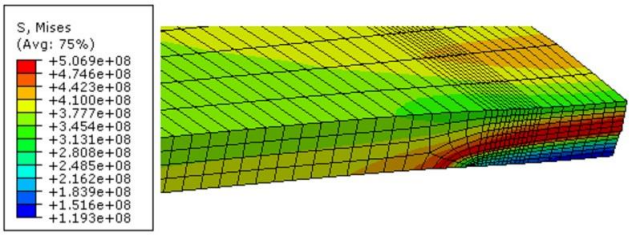

Fig.8
Stress distribution near the crack edge (3rd experiment).

Horizontal and vertical axes of failure assessment diagram are obtained by dividing stress intensity factor to fracture toughness and the reference stress to yield stress. In this study, the amounts of K_r and L_r which are calculated and shown in Table 5, are two parameters that are going to be minimized. According to Taguchi method, a multi-objective optimization is needed. First, loss function for each objective is calculated using Eq. (12) (related to the lower-is-better case). Then, loss functions are normalized by dividing them to the maximum amount of loss function. Moreover, an equivalent loss function is obtained by contributing appropriate weight to each output (Eq. (13)). Finally, the amount of signal to noise ratio (SN ratio) is obtained for each experiment (Eq. (14)).

$$L_i = \frac{1}{n}\sum y_i^2 \tag{12}$$

where n is the number of trials in the experiment and y is the amount of desired output.

$$L_{Equivalent} = W_1 L_1 + W_2 L_2 \tag{13}$$

$$SN = -10\log(L_{Equivalent}) \tag{14}$$

So, the procedure of obtaining optimum levels are as follows:

- Calculating loss function for each output.
- Normalizing loss function for each output.
- Calculating equivalent loss function for each experiment by assigning appropriate weights.
- Calculating signal to noise ratio for each experiment and obtaining mean value of SN ratio for every levels for each parameter.

Loss functions, their normalized amounts and SN ratios are calculated and shown in Table 5. and the distribution of scattered data of finite element results are shown in Fig. 9 in comparison with the failure assessment diagram. Fig. 9 shows that, the effect of minimum the amount of L_r in making safe condition is more than minimum the

amount of K_r . So the weight coefficients are considered as 0.3 and 0.7 for K_r and L_r , respectively. As it can be seen from Fig. 9, most of failure in experiments belong to ductile failure.

Table 5
Multi-objective Taguchi table for obtaining SN ratios.

Number	L_r	K_r	Loss function L_r	Loss function K_r	Normalized loss function L_r	Normalized loss function K_r	$L_{Equvalent}$	SN ratio
1	0.6793	0.11	0.4614	0.0121	0.1851	0.0598	0.1475	8.3121
2	0.8851	0.2	0.7834	0.04	0.3143	0.1975	0.2793	5.5393
3	1.0837	0.25	1.1744	0.0625	0.4712	0.3086	0.4224	3.7428
4	1.2768	0.37	1.6302	0.1369	0.6540	0.6760	0.6606	1.8006
5	0.6640	0.43	0.4409	0.1849	0.1769	0.9131	0.3978	4.0034
6	0.9495	0.19	0.9016	0.0361	0.3617	0.1783	0.3067	5.1329
7	1.0681	0.27	1.1408	0.0729	0.4577	0.3600	0.4284	3.6815
8	1.3863	0.4	1.9218	0.16	0.7710	0.7901	0.7767	1.0975
9	0.8310	0.15	0.6906	0.0225	0.2770	0.1111	0.2272	6.4359
10	0.6669	0.16	0.4448	0.0256	0.1784	0.1264	0.1628	7.8835
11	1.4487	0.43	2.0987	0.1849	0.8420	0.9131	0.8633	0.6384
12	1.3439	0.45	1.8061	0.2025	0.7284	1	0.8072	0.9302
13	0.8805	0.18	0.7753	0.0324	0.3110	0.16	0.2657	5.7561
14	0.6530	0.13	0.4264	0.0169	0.1711	0.0835	0.1448	8.3923
15	1.5788	0.43	2.4926	0.1849	1	0.9131	0.9739	0.1149
16	1.3182	0.36	1.7393	0.1296	0.6978	0.64	0.6805	1.6717
17	1.2063	0.23	1.4552	0.0529	0.5838	0.2612	0.4870	3.1247
18	1.0616	0.26	1.1270	0.0676	0.4521	0.3338	0.4166	3.8028
19	0.9059	0.22	0.8272	0.0484	0.3319	0.2390	0.3040	5.1713
20	0.7370	0.23	0.5432	0.0529	0.2179	0.2612	0.2309	6.3658
21	1.2748	0.33	1.6251	0.1089	0.6520	0.5378	0.6177	2.0922
22	1.0423	0.23	1.0864	0.0529	0.4358	0.2612	0.3834	4.1635
23	0.9827	0.23	0.9657	0.9657	0.3874	0.2612	0.3495	4.5655
24	0.7295	0.19	0.5322	0.5322	0.2135	0.1783	0.2029	6.9272
25	1.1789	0.23	1.3898	1.3898	0.5576	0.2612	0.4687	3.2911
26	1.3951	0.43	1.9463	1.9463	0.7808	0.9131	0.8205	0.8592
27	0.6898	0.16	0.4758	0.0256	0.1909	0.1264	0.1715	7.6574
28	0.9124	0.27	0.8325	0.0729	0.3340	0.36	0.3418	4.6623
29	1.1492	0.25	1.3207	0.0625	0.5298	0.3086	0.4634	3.3404
30	1.5021	0.44	2.2563	0.1936	0.9052	0.9560	0.9204	0.3602
31	0.6771	0.17	0.4585	0.0289	0.1839	0.1427	0.1715	7.6574
32	0.9957	0.32	0.9914	0.1024	0.3977	0.5057	0.4301	3.6643

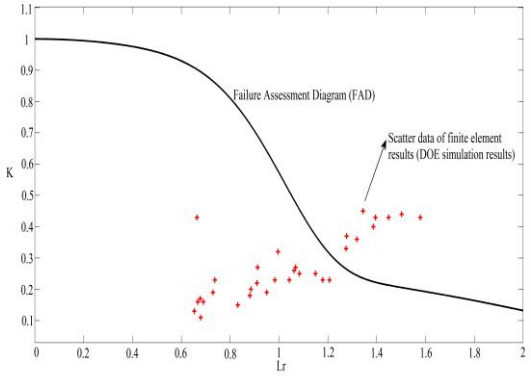

Fig.9
Finite element results for 32 Taguchi experiments and a comparison to FAD.

Fig. 10 shows the mean of SN ratios for each level of parameters. For example, mean value of SN ratio for the first level of crack length is calculated by averaging all SN ratios which crack length is in its first level. According to Fig. 10, the level which has the maximum amount of SN ratio is the optimum case to minimize the equivalent loss function and results the safest working condition on FAD. So, crack depth, crack length, crack position, internal pressure and pipe thickness are minimum in their 1st, 1st, 2nd, 1st and 4th levels, respectively. Besides that, it can be concluded that equivalent loss function and FAD working condition decreases as crack depth increases. The

behavior of crack length is the same as crack depth's variation (Fig. 10). Comparing mean of SN ratio for internal and external crack position shows that external crack position is the optimum case. Finally, it is observed that the equivalent loss function increases as the internal pressure rises.

Lastly, a finite element modeling and analysis is carried out based on optimum levels of the parameters in order to verify. The amount of equivalent loss function and its corresponding SN ratio are 0.44 and 3.5655, respectively. The error between mean of SN ratios among all 32 experiments and the optimum case is 4.5%. This error percent shows that the optimization process is acceptable. L_r and K_r are computed as 0.082 and 0.264, respectively. If coordinates of the optimum working condition points are compared with the scatter data in Fig. 9, it can be concluded that the optimum case is in a very safe condition and far from the scatter data and shows the efficiency of the optimization procedure. The summary of optimized parameter levels are as follows:

- Crack depth (level 1: 5mm)
- Crack length (level 1: 100mm)
- Crack position (level 2: external)
- Internal pressure (level 1: 3MPa)
- Pipe thickness (level 4: 15mm)

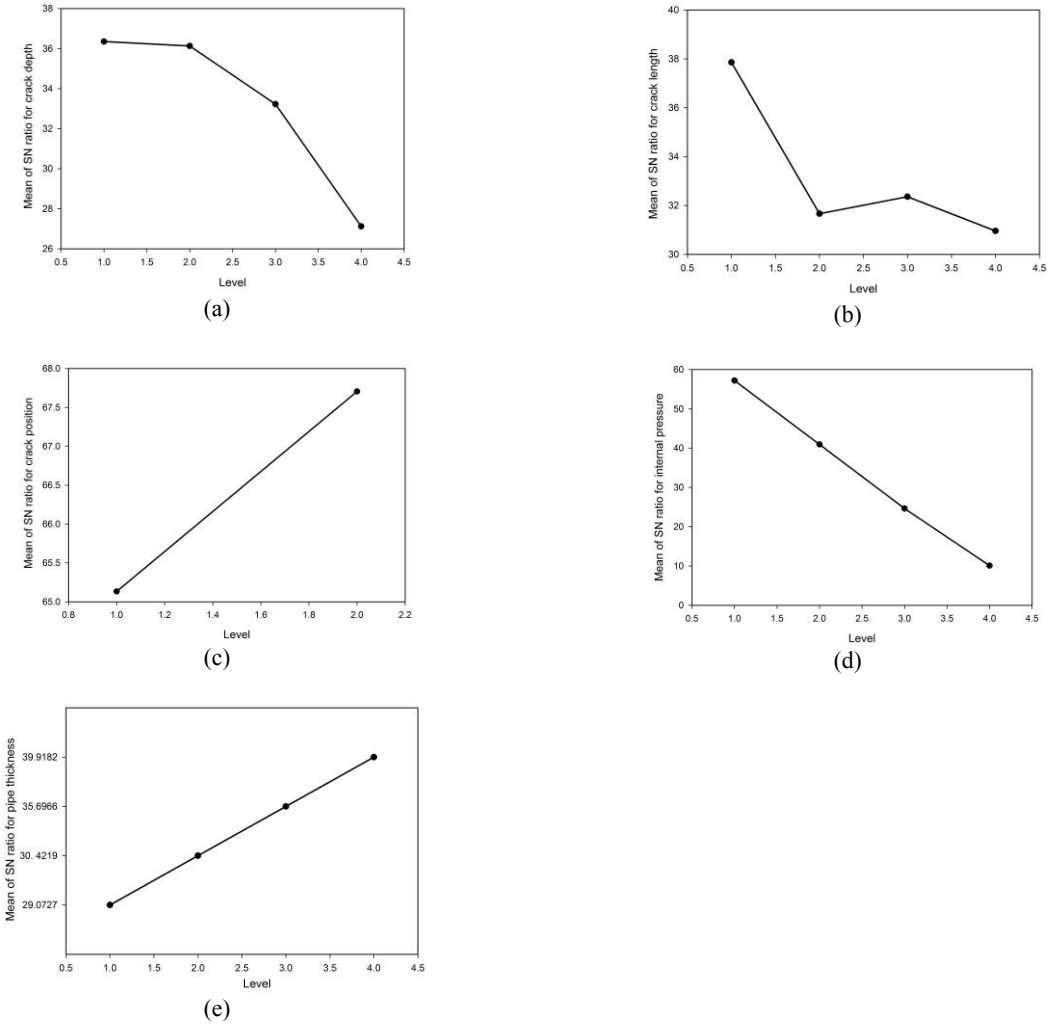

Fig.10
Mean value of SN ratios in different levels for (a) Crack depth, (b) Crack length, (c) Crack position, (d) Internal pressure, (e) Pipe thickness.

Fig. 11 shows a comparison between experiments 18, 22 and 25 and two others that has close parameter levels to the optimum case. These two new experiments are as follows:

- First case: crack depth: 5mm, crack length: 100, crack place: external, internal pressure: 3MPa, pipe thickness: 13*mm*.
- Second case: crack depth: 5mm, crack length: 100mm, crack place: external, internal pressure: 4MPa, pipe thickness: 14*mm*.

It can be inferred that the more designing parameters close to the optimum case, the more possibility to have a safer failure condition (Fig. 11).

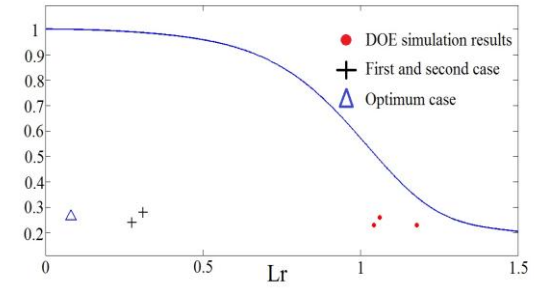

Fig.11
Comparison between optimum case, DOE simulation results and two other close cases to the optimum case.

5 VERIFICATION

An experimental study is conducted on steel natural gas pipeline of API X65-grade and the results are plotted in failure assessment diagram (FAD) [5]. Pipe diameter and thickness are considered as 762 *mm* and 17.5 *mm* reported experimental study [5]. So, a finite element modeling is performed under the same dimensions. The experimental investigation is done on different crack depths (10, 12, 13 and 14 *mm*). Fig. 12 shows a comparison between experimental and numerical results for the reference stress and stress intensity factor for a longitudinal semi-elliptical crack in a natural gas pipeline. It is visible that a good agreement is achieved between numerical and experimental results.

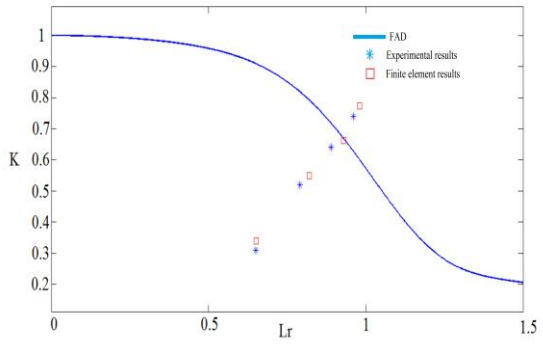

Fig.12
Comparison between numerical and experimental results for a longitudinal semi-elliptical crack for the base metal in natural gas pipeline.

6 CONCLUSIONS

In this paper, a three dimensional finite element analysis is conducted in order to study and optimize the safety and failure of gas pipeline. Effect of crack position, crack length, crack depth, internal pressure and pipe thickness are taken into account for semi-elliptical crack by implementing finite element analysis. Then, by using design of experiments (DOE), 32 finite element simulations are designed and carried out to calculate *J* integrals. In continue, by using the multi-objective Taguchi method, the working condition coordinates of failure assessment diagram (FAD) are compared and optimized to be minimum and in the safest condition. The comparison between the results of optimum design and other DOE results has shown that the optimum case has the safest condition and is far from

ductile failure. The optimum levels of each parameter and also the optimum pipe design are obtained and the changes in FAD working condition coordinates according to the changes in parameters are found. It is also shown that the more design parameters close to the optimum case, the safer condition is achieved for the pipe. Finally, a verification study is performed on FAD working condition coordinates for a longitudinal semi-elliptical crack in a natural gas pipeline and a good agreement is found between the finite element and experimental results.

REFERENCES

[1] Underwood J.H., 1972, Stress intensity factors for internally pressurized thick-walled cylinders*, American Society for Testing and Materials* **513** : 59-70.

[2] Raju I.S., Newman J.C., 1980, Stress-intensity factors for internal and external surface cracks in cylindrical vessels, *Journal of Pressure Vessel Technology* **102**(4): 293-298.

[3] Newman J.C., 1976, Fracture analysis of surface and through cracks in cylindrical pressure vessels, *National Aeronautics and Space Administration* **39***:* 21-33.

[4] Liu A., 1996, *Rockwell International Science Center*, ASM Handbook Fatigue and Fracture.

[5] Lee S.L., Ju J.B., Kim W.S., Kwon D., 2004, Weld crack assessments in API X65 pipeline: failure assessments diagrams with variations in representative mechanical properties, *Materials Science and Engineering* **373**(1): 122-130.

[6] Oh C.K, Kim Y.J, Baek J.H., Kim Y.P., Kim W.S., 2007, Ductile failure analysis of API X65 pipes with notch-type defects using a local fracture criterion, *International Journal of Pressure Vessels and Piping* **84**: 512-525.

[7] Sandvik A., Ostby E., Thaulow C., 2008, A probabilistic fracture mechanics model including 3D ductile tearing of bi-axially loaded pipes with surface cracks, *Engineering Fracture Mechanics* **75**: 76-96.

[8] Pluvinage G., Capelle J., Schmitt G., Mouwakeh M., 2012, Doman failure assessment diagrams for defect assessment of gas pipes, *19th European Conference on Fracture*, Kazan, Russia.

[9] Zhang B., Ye C., Liang B., Zhang Z., Zhi Y., 2014, Ductile failure analysis and crack behavior of X65 buried pipes using extended finite element method, *Engineering Failure Analysis* **45**: 26-40.

[10] Ghajar R., Mirone G., Keshavarz A., 2013, Ductile failure of X100 pipeline steel-Experiments and fractography, *Materials & Design* **43**: 513-525.

[11] Sharma K., Singh I.V., Mishra B.K., Maurya S.K., 2014, Numerical simulation of semi-elliptical axial crack in pipe bend using XFEM, *Journal of Solid Mechanics* **6**(2): 208-228.

[12] Dimic I., Medjo B., Rakin M., Arsic M., Sarkocevic Z., Sedmak A., 2014, Failure prediction of gas and oil drilling rig pipelines with axial defects, *Procedia Materials Science* **3**: 955-960.

[13] Ainsworth R.A., 1984, The assessment of defects in structures of strain hardening material, *Engineering Fracture Mechanics* **19**(4):633-642.

[14] Anderson T.L., Osage D.A., 2000, API 579: a comprehensive fitness-for-service guide , *International Journal of Pressure Vessels and Piping* **77**(14):953-963.

[15] API 579*, 2000, Recommended Practice for Fitness for Service*, American Petroleum Institute.

[16] BS7910, 1999, *Guide and Methods for Assessing the Acceptability of Flaws in Fusion Welded Structures*, British Standard Institutions.

[17] R-6,1998, *Assessment of the Integrity of Structures Containing Defects*, British Energy.

[18] BS EN ISO 7448, 1999, Metallic Materials Determination of Plan-Strain Fracture Toughness, British Standard Institution.

[19] Shahraini S.I., Hashemi S.H., 2014, Effects of surface crack length and depth variations on gas transmission pipeline safety, *Modares Mechanical Engineering* **14***:*26-32.

[20] Habbit, Karlsson, Sorensen, 2007, Abaqus/Standard Analysis User's Manual, USA.